Computer Assisted Mechanics and Engineering Sciences, 8: 289–311, 2001.

Developments with hybrid-Trefftz stress and displacement elements

João A. Teixeira de Freitas and Corneliu Cismaşiu
Departamento de Engenharia Civil e Arquitectura, Instituto Superior Técnico
Universidade Técnica de Lisboa, 1049-001 Lisboa, Portugal

(Received June 30, 2000)

The paper reports on the work on hybrid-Trefftz finite elements developed by the Structural Analysis Research Group, ICIST, Technical University of Lisbon. A dynamic elastoplastic problem is used to describe the technique used to establish the alternative stress and displacement models of the hybrid-Trefftz finite element formulations. They are derived using independent time, space and finite element bases, so that the resulting solving systems are symmetric, sparse, naturally p-adaptive and particularly well suited to parallel processing. The performance of the hybrid-Trefftz stress and displacement models is illustrated with a number of representative static and dynamic applications of elastic and elastoplastic structural problems.

Keywords: Hybrid-Trefftz elements, elasticity, elastoplasticity, dynamics

1. Introduction

The research developed by the Structural Analysis Group is focused on the development, implementation and testing of hybrid variants of the finite element method. It depends strongly, therefore, on the definition of a well-structured classification of the many variants available and on a clear identification of the interrelationships that may exist.

This work, which has been developed from the ideas originally proposed by J. Munro and D.L. Smith [51], led to the identification of the following basic guidelines [20]: to depart from the relevant first principles of mechanics; to discard the node concept in favour of generalised variables; to enforce energetically consistent definitions for the discrete generalised variables; to process the alternative finite element formulations through mathematical programming.

Development of the finite element formulations from first principles is used to release the approach from the assumptions implied in the existing variational approaches, to identify clearly how each condition is being enforced and, also, to strengthen the flexibility in the development of alternative formulations and models.

The use of generalised variables in detriment of the node concept is justified by the objective of exploiting fully the use of naturally hierarchical approximation functions and of alternative Galerkin and collocation methods in the enforcement of the structural conditions.

Consistency of the formulations is an essential ingredient of the development. Duality is used to ensure the supporting condition on the invariance of the inner product in all finite element mappings and thus preserve the fundamental properties of the continuum in its discrete model.

Mathematical programming is called upon to recover the associated variational theorems, to establish the conditions for the existence, uniqueness and stability of the solutions and, eventually, to design appropriate solution procedures.

The implementation of this approach led to the identification of three classes of finite element formulations, namely the hybrid-mixed, hybrid and hybrid-Trefftz formulations, and to the definition of two alternative models for each formulation, the stress model and the displacement model.

The following terminology is used here: an element is said to be hybrid if it involves the independent approximation of at least one field in its domain and, simultaneously, at least one field on its boundary; an element is said to be mixed if it develops from the direct approximation of at least two fields in its domain; a Trefftz element is characterised by domain approximations that solve locally all domain conditions of the problem; and an element is said to be a displacement (stress) element if the inter-element continuity condition is enforced in terms of conformity of displacements (diffusivity of stresses).

As research on this topic developed, it became clear that these alternative finite element formulations constitute an ordered and interrelated sequence, instead of representing independent and apparently unrelated approaches to the finite element method.

The hybrid-mixed formulation is considered to be the most general, in the sense that the domain approximations are not constrained to satisfy a priori the domain conditions of the problem. The displacement (stress) model of the hybrid formulation can be obtained from the displacement (model) of the hybrid-mixed formulation simply by constraining the displacement (stress) approximation to satisfy locally the compatibility (equilibrium) condition in the domain of the element. If this model is constrained to satisfy also the equilibrium (compatibility) condition and the constitutive relations in the domain of the element, the displacement (stress) model of the hybrid finite element formulation collapses into the equivalent model of the hybrid-Trefftz formulation.

The involvement of the group with Trefftz-type elements happened before this framework had been established and it was motivated by attempts to reassess the basic ideas that support the development of the competing boundary element method. The discretisation criteria that destroyed the fundamental properties of the problem being modelled, namely symmetry, were the first issue that was addressed [13–16]. The understanding that it was the use of fundamental solutions that led to boundary integral expressions for the structural matrices suggested the following step of using regular solutions of the problem to overcome all difficulties associated with singular and hypersingular integrals [34]. Only later was it realised that the approaches that were being followed corresponded to the encodement of the Trefftz method in a modern finite element format, as it had been suggested by J. Jirousek [38, 39]. The concepts and the procedures that are shared and those that distinguish these approaches are commented and assessed in [17, 25, 26].

To clarify the approach reported here, the alternative displacement and stress models of the hybrid-Trefftz finite element formulation are derived here using elastoplastic dynamics as the supporting application. The applications that have been implemented and tested are summarised next. The paper closes with the presentation of a selected number of testing problems.

2. FUNDAMENTAL RELATIONS

Let V represent the domain and Γ the enveloping surface of the element, referred to a Cartesian coordinate system. Let further $V_P \subseteq V$ define the sub-domain where plastic strains may develop and denote by Γ_P its envelope. The fundamental relations governing dynamic elastoplastic problems can be summarised as follows, where t is the time parameter,

$$\boldsymbol{\mathcal{D}\sigma} = \boldsymbol{\rho\ddot{u}} \qquad \text{in } V, \tag{1}$$

$$\boldsymbol{\varepsilon}_E + \boldsymbol{\varepsilon}_P = \boldsymbol{\mathcal{D}}^* \boldsymbol{u}, \qquad \text{in } V \tag{2}$$

$$\boldsymbol{\sigma} = \boldsymbol{k\varepsilon}_E + \boldsymbol{c\dot{\varepsilon}}_E \qquad \text{in } V, \tag{3}$$

$$\boldsymbol{N\sigma} = \boldsymbol{t}_\Gamma \qquad \text{on } \Gamma_\sigma, \tag{4}$$

$$\boldsymbol{u} = \boldsymbol{u}_\Gamma \qquad \text{on } \Gamma_u, \tag{5}$$

$$\boldsymbol{u}(t{=}0) = \boldsymbol{u}_0 \quad \text{and} \quad \dot{\boldsymbol{u}}(t{=}0) = \dot{\boldsymbol{u}}_0 \qquad \text{in } V, \tag{6}$$

$$\Phi_* \leq 0 \qquad \text{in } V_P, \tag{7}$$

$$\Phi_* = \varphi(\boldsymbol{\sigma}) - \boldsymbol{h\varepsilon}_* + \nabla^T \boldsymbol{\sigma}_* - \Phi_0 \qquad \text{in } V_P, \tag{8}$$

$$n^T \boldsymbol{\sigma}_* = \boldsymbol{\sigma}_{*\Gamma} \quad \text{on } \Gamma_{\sigma P}, \tag{9}$$

$$\dot{\boldsymbol{\varepsilon}}_* \geq 0 \quad \text{in } V_P, \tag{10}$$

$$\dot{\boldsymbol{\varepsilon}}_P = \nabla_\sigma \boldsymbol{\varphi}(\boldsymbol{\sigma}) \dot{\boldsymbol{\varepsilon}}_* \quad \text{in } V_P, \tag{11}$$

$$\boldsymbol{\gamma}_* = \nabla \boldsymbol{\varepsilon}_* \quad \text{in } V_P, \tag{12}$$

$$\boldsymbol{\varepsilon}_* = \boldsymbol{\varepsilon}_{*\Gamma} \quad \text{on } \Gamma_{uP}, \tag{13}$$

$$\boldsymbol{\sigma}_* = \boldsymbol{c}_* \boldsymbol{\gamma}_* \quad \text{in } V_P, \tag{14}$$

$$\boldsymbol{\Phi}_*^T \dot{\boldsymbol{\varepsilon}}_* = 0 \quad \text{and} \quad \dot{\boldsymbol{\Phi}}_*^T \dot{\boldsymbol{\varepsilon}}_* = 0 \quad \text{in } V_P, \tag{15}$$

$$\left(\boldsymbol{n}^T \boldsymbol{\sigma}_*\right)^T \boldsymbol{\varepsilon}_* = 0 \quad \text{on } \Gamma_P. \tag{16}$$

Equations (1) to (6) define elastodynamic problems and conditions (7) to (16) correspond to the description used in [35] of the gradient-dependent (non-local) plasticity model proposed by Mühlhaus and Aifantis [50].

In the conditions of equilibrium (1) and compatibility (2), vector $\boldsymbol{\sigma}$ lists the independent components of the stress tensor, vector $\boldsymbol{\varepsilon} = \boldsymbol{\varepsilon}_E + \boldsymbol{\varepsilon}_P$ defines the corresponding components of the elastic-plastic strain tensor and vectors $\boldsymbol{u}$, $\dot{\boldsymbol{u}}$ and $\ddot{\boldsymbol{u}}$ define the displacement, velocity and acceleration fields, respectively. In Eq. (1), where the body force term is removed for simplicity, $\boldsymbol{\rho}$ is the specific mass matrix. As a geometrically linear model is assumed, the differential equilibrium and compatibility operators $\boldsymbol{\mathcal{D}}$ and $\boldsymbol{\mathcal{D}}^*$ are linear and adjoint.

In description (3) for the elasticity condition, matrices $\boldsymbol{k}$ and $\boldsymbol{c}$ collect the relevant elastic and material damping constants, respectively.

Equations (4) to (6) define the boundary and initial conditions of the problem. In the Neumann boundary condition (4), the stress vector $\boldsymbol{t}_\Gamma$ defines the tractions prescribed on portion Γ_σ of the boundary and the boundary equilibrium matrix $\boldsymbol{N}$ collects the components of the unit outward normal vector associated with the differential operators present in the domain equilibrium matrix $\boldsymbol{\mathcal{D}}$. In the Dirichlet boundary condition (5), vector $\boldsymbol{u}_\Gamma$ defines the displacements prescribed on the complementary portion of the boundary, Γ_u. Mixed boundary conditions are assumed to be accounted for in the usual notation for geometric complementarity: $\Gamma = \Gamma_\sigma \cup \Gamma_u$; $\emptyset = \Gamma_\sigma \cap \Gamma_u$.

The initial conditions (6) are expressed in terms of initial displacements and velocities, $\boldsymbol{u}_0$ and $\dot{\boldsymbol{u}}_0$; alternative initial conditions can be easily accommodated.

The yield condition (7), the definition (8) for the yield function and the boundary condition (9) on the plastic radiation vector, $\boldsymbol{\sigma}_*$, characterise the static phase of plasticity. Vector $\boldsymbol{\varphi}(\boldsymbol{\sigma})$ is the effective stress vector, $\boldsymbol{h}$ is the hardening matrix, $\boldsymbol{\varepsilon}_*$ is the plastic multiplier vector, $\boldsymbol{\Phi}_o$ is the initial yield limit vector, ∇ is the gradient vector and $\boldsymbol{n}$ is the associated unit outward normal vector.

In the dual description of the kinematic phase of plasticity, condition (10) defines the flow rule, Eq. (11) constrains the plastic deformation rates to be orthogonal to the yield surface, Eq. (12) defines the associated plastic multiplier gradient vector, $\boldsymbol{\gamma}_*$, and Eq. (13) defines the boundary condition on the plastic multiplier rates.

The plastic association conditions are represented by Eq. (14), where matrix $\boldsymbol{c}_*$ collects the relevant plastic diffusion parameters, and by the complementarity conditions (15) and (16) respectively on the plastic potential and plastic parameter vectors and on the plastic radiations and plastic parameter gradients.

Mixed boundary conditions on the rates of plastic radiation and on the plastic multiplier fields are accepted in descriptions (9) and (13), where the usual notation for geometric complementarity is again assumed to hold: $\Gamma_P = \Gamma_{\sigma P} \cup \Gamma_{uP}$; $\emptyset = \Gamma_{\sigma P} \cap \Gamma_{uP}$.

It is stressed that the variables, arrays and operators are identified above in the generalised sense, meaning that the fundamental conditions (1) to (16) hold for alternative linear, laminar and three-dimensional structural models. They may also be used to represent non-structural problems, for instance the standard potential problems associated with the Poisson equation. The equations above

are constrained to geometrically linear problems but they hold for the analysis of inhomogeneous and multiphase physically linear or non-linear media.

3. Time and space discretisation

The first step in the solution of structural dynamics problems consists in implementing a time discretisation procedure, in either the time or the frequency domains. This discretisation is applied directly to system (1)–(16) and the resulting equations are then subject to the space discretisation and the finite element approximation described below.

As it will become apparent, the approximation of the structural fields is implemented on hierarchical bases. This implies that the finite element variables are generalised (non-nodal) variables that, in general, cannot be identified directly with physical quantities like stresses, forces, strains or displacements. This loss in the immediate interpretation of the finite element variables is compensated by the possibility of exploiting hierarchical and naturally adaptive solution schemes and, also, the implementation of the solving systems in parallel processing mode [8].

Yet another advantage of using generalised finite element variables is the possibility of using approximations for the structural fields completely independent of the description of the geometry of the finite element mesh. Consequently, the finite element models described below can be implemented on coarse meshes of super-elements, each of which may have a different geometry in terms of number and shape of sides. In particular, these elements may not be convex, simply connected or bounded.

The space discretisation technique used is described, for instance, in [25]. It consists in establishing the geometry of the meshes through the coordinates of master nodes. The definition of the lines (surfaces) of a two- (three-) dimensional mesh is established by assigning the master nodes and a parametric (polynomial, spline, trigonometric or other) description to each line or surface. Finally, the domain of each finite element is identified by its bounding lines or surfaces. At the cost of loosing flexibility in shape description, it is possible, also, to implement the finite element models described here on meshes obtained with the geometric mappings typical of iso-parametric displacement elements, as processed by the mesh generators available in commercial codes.

4. Finite element approximations

The stress model of the hybrid-Trefftz formulation is based on the direct approximation of the stresses in the domain of the element and of the displacements on its static (Neumann) boundary,

$$\boldsymbol{\sigma} = \boldsymbol{S}_V \boldsymbol{X}_V \qquad \text{in } V, \tag{17}$$

$$\boldsymbol{u} = \boldsymbol{U}_\Gamma \boldsymbol{q}_\Gamma \qquad \text{on } \Gamma_\sigma . \tag{18}$$

Complementary, the displacement model of the hybrid-Trefftz formulation is based on the direct approximation of the displacements in the domain of the element and of tractions on its kinematic (Dirichlet) boundary,

$$\boldsymbol{u} = \boldsymbol{U}_V \boldsymbol{q}_V \qquad \text{in } V, \tag{19}$$

$$\boldsymbol{t} = \boldsymbol{S}_\Gamma \boldsymbol{X}_\Gamma \qquad \text{on } \Gamma_u . \tag{20}$$

It is recalled that the static (kinematic) boundary of a hybrid stress (displacement) element is understood as the portion of its boundary whereon the displacements (tractions) are not known. Besides all inter-element boundaries, it includes the natural Neumann (Dirichlet) boundary of the mesh that the stress (displacement) element may contain.

In the Trefftz approach, the stress and displacement approximation bases $\boldsymbol{S}_V$ and $\boldsymbol{U}_V$ are derived from the (hierarchical) solution sets of the homogeneous governing differential equation written in terms of stress and displacement potentials, respectively. Because the node concept is not called

upon, variables $\boldsymbol{X}_V$ and $\boldsymbol{q}_V$ represent generalised stresses and displacements, respectively. Definitions (17) and (19) can be extended to include vectors $\boldsymbol{\sigma}_0$ and $\boldsymbol{u}_0$, respectively, which are used as particular solutions associated, for instance, with body forces and local static and kinematic boundary conditions.

Similarly, in the boundary approximation Eqs. (18) and (20) vectors $\boldsymbol{q}_\Gamma$ and $\boldsymbol{X}_\Gamma$ represent generalised displacements and tractions, respectively, as matrices $\boldsymbol{U}_\Gamma$ and $\boldsymbol{S}_\Gamma$ collect the (orthogonal, hierarchical) approximation functions.

The complementary and particular bases used in the implementation of hybrid-Trefftz elements for potential problems and two- and three-dimensional elastostatic and elastodynamic problems can be found, for instance, in [7, 17, 21, 25, 34, 55].

The elastoplastic applications reported below are based on the hybrid-Trefftz stress model. A plastic cell mesh is superimposed onto the finite element mesh where approximations (17) and (18) hold and the plastic multiplier and plastic radiation fields are approximated independently in the domain and on the boundary of each plastic cell,

$$\boldsymbol{\varepsilon}_* = \boldsymbol{E}_* \boldsymbol{e}_* \qquad \text{in } V_P\,, \tag{21}$$

$$\boldsymbol{\sigma}_* = \boldsymbol{S}_* \boldsymbol{X}_* \qquad \text{in } \Gamma_{uP}\,. \tag{22}$$

Approximation (22) is discarded in the implementation of local plasticity models. As before, hierarchical bases can be used and the associated finite element variables $\boldsymbol{e}_*$ and $\boldsymbol{X}_*$ represent non-nodal, generalised plastic multipliers and radiations. The plasticity bases used in two- and three-dimensional applications are reported in [3, 4, 35, 36, 55].

5. Derivation of the finite element equations

Different techniques can be used to establish the finite element equations that result from the fundamental approximations (17) to (22).

The approach most commonly used consists in condensing system (1)–(16) in a set of selected independent variables, frequently the displacements and the plastic multipliers. The major disadvantage this approach suffers from is that this elimination is attained by assuming that specific domain conditions are locally satisfied by the finite element approximations, and thus restricts a priori the scope of the formulation.

A second approach frequently used is the derivation of the finite element equations from an existing or newly coined variational statement. The scope of the resulting finite element formulation is relatively wider but it still shares the problem-dependency limitation. The derivation of new variational statements for a given problem and for a given approximation criterion may not be a simple task in what concerns consistency.

To overcome the difficulties and limitations mentioned above, the duality approach suggested originally by Munro and Smith [51] has been applied in the derivation of the alternative stress and displacement models of the hybrid-Trefftz finite element formulation reported here. Besides ensuring consistency by preserving the invariance of the inner product in the finite element mappings (17) to (22), this approach leads to the definition of the finite element description of each of the fundamental equations and conditions present in system (1)–(16). The resulting finite element formulation is rather more flexible, and thus less problem-dependent. Extensions are implemented by adding new equations and conditions, or new terms to the formulation established previously, for instance those associated with structural damping or residual stresses and strains in system (1)–(16). On the other hand, particularisation is implemented simply by removing the irrelevant equations and variables. For instance, the plastic-limit analysis problem is recovered by deleting all terms associated with elasticity in system (1)–(16).

The issue of establishing the variational statements associated with the newly developed finite element formulation is solved a posteriori by interpreting the finite element solving system as a Karush–Kuhn–Tucker problem. The associated mathematical programs are established using

standard mathematical programming equivalence criteria and interpreted physically to establish the variational interpretation. They are also processed through well-established mathematical programming qualification theorems to define sufficient conditions for the existence, uniqueness, multiplicity and stability of the finite element solutions. See, for instance, [13, 14, 17].

In this approach, the development of the finite element formulation results directly from the dual statements (23)–(28) of the fundamental approximations (17)–(22),

$$\boldsymbol{e}_V = \int \boldsymbol{S}_V^T \boldsymbol{\varepsilon} \, \mathrm{d}V, \tag{23}$$

$$\boldsymbol{Q}_\Gamma = \int \boldsymbol{U}_\Gamma^T \boldsymbol{t}_\Gamma \, \mathrm{d}\Gamma_\sigma \,, \tag{24}$$

$$\boldsymbol{Q}_V = \int \boldsymbol{U}_V^T \boldsymbol{b} \, \mathrm{d}V, \tag{25}$$

$$\boldsymbol{e}_\Gamma = \int \boldsymbol{S}_\Gamma^T \boldsymbol{u}_\Gamma \, \mathrm{d}\Gamma_u \,, \tag{26}$$

$$\boldsymbol{\varphi}_* = \int \boldsymbol{E}_*^T \boldsymbol{\Phi}_* \, \mathrm{d}V_P \,, \tag{27}$$

$$\boldsymbol{e}_{*\Gamma} = \int \boldsymbol{S}_{*\Gamma}^T \boldsymbol{\varepsilon}_{*\Gamma} \, \mathrm{d}\Gamma_{uP} \,. \tag{28}$$

The equations above define the generalised strains, tractions, body-forces, boundary displacements, plastic potentials and boundary plastic multipliers consistent with the finite element approximations (17) to (22), in the sense that the finite element variables dissipate the same energy as the continuum variables they represent. For instance, for the dual pair of generalised stresses and strains, definitions (17) and (23) yield the following invariance condition on the inner product of the associated finite element mapping,

$$\boldsymbol{X}_V^T \boldsymbol{e}_V = \int \boldsymbol{\sigma}^T \boldsymbol{\varepsilon} \, \mathrm{d}V. \tag{29}$$

Similar expressions can be found for the dual finite element pairs of variables $\{\boldsymbol{Q}_\Gamma \,, \boldsymbol{q}_\Gamma\}$, $\{\boldsymbol{Q}_V \,, \boldsymbol{q}_V\}$, $\{\boldsymbol{X}_\Gamma \,, \boldsymbol{e}_\Gamma\}$, $\{\boldsymbol{\varphi}_* \,, \boldsymbol{e}_*\}$ and $\{\boldsymbol{X}_* \,, \boldsymbol{e}_{*\Gamma}\}$.

As it has been stated above, Eqs. (23) to (28) and the assumed Trefftz constraint on the finite element domain approximations establish the framework and the guidelines necessary to derive the alternative stress and displacement models of the hybrid-Trefftz finite element formulation. For instance, the derivation of the stress model develops as follows, e.g. [17, 19, 35]:

a) Use definition (23) for the generalised strains to enforce independently and on average, in the sense of Galerkin, the compatibility condition (2). Integrate by parts the resulting equation to enforce locally condition (5) on the Dirichlet boundary and the boundary displacement approximation (18) on the Neumann boundary of the element.

b) Use definition (24) for the generalised tractions to enforce on average condition (4) on the Neumann boundary of the element for the assumed stresses (17). It is recalled that this approximation, and the implied approximation for the inertia forces, e.g. [18, 19], is constrained a priori to satisfy locally equilibrium condition (1).

c) Use definition (23) for the generalised strains to enforce on average the (flexibility version of the) elasticity condition (3) for the assumed stresses (17).

d) Use the same definition to enforce on average the plastic flow condition (9) for the assumed plastic multiplier field (21).

e) Use definition (27) for the generalised plastic potentials to enforce on average the plastic yield and diffusivity conditions (7), (8) and (14) for the assumed stresses (17) and plastic multipliers (21). Integrate by parts the resulting equation to enforce locally the plastic gradient definition (12), the static boundary condition (9) on the Neumann boundary of the plastic cells and the plastic radiation approximation (22) on their Dirichlet boundary.

f) Use definition (28) for the generalised boundary plastic multipliers to enforce on average the Dirichlet condition on the plastic cells for the assumed plastic multipliers (21).

The derivation of the displacement model of the hybrid-Trefftz finite element formulation is in every aspect complementary to the procedure described above. In both cases, the process is concluded by enforcing the Trefftz constraint on the domain approximations to obtain boundary integral expressions for all finite element matrices associated with material properties.

6. Applications with hybrid-Trefftz elements

The strongest limitation in the implementation of hybrid-Trefftz elements is the fulfilment of the Trefftz constraint, that is the condition that the domain approximation basis must be extracted from the solution set of the differential equations governing the problem being analysed. The derivation of such bases may not be trivial, particularly in the solution of non-linear problems. However, once these bases are secured, the advantages offered by Trefftz elements are difficult to surpass as they combine the major features of the competing finite element and boundary element methods.

The approximation bases are built on regular and naturally hierarchical series, but they may be enriched to include the modelling of local effects with a strong influence on the rate of convergence. The solving system preserves the fundamental properties of the continuum problem, namely symmetry, and are sparse, free of spurious modes and well conditioned, with the advantage that all matrices and vectors present in that system are defined by boundary integral expressions. Moreover, the richness in information on the mechanics of the problem being modelled enhances high accuracy with relatively few degrees of freedom.

The efficiency that can be attained in the storage and solution of such systems is countered by the implementation of the heavy procedures required to process the singular functions that may be included in the approximation bases to model local effects. Analytical and semi-analytical integration procedures seem to be the natural way to overcome this difficulty, exploiting the currently available symbolic processing programs.

The stress and displacement models described succinctly above have been applied to the solution of potential problems, [17, 25, 26], to characterise and assess the relative performance of the alternative stress, displacement and least-square models of the hybrid-Trefftz finite element formulation presented in the literature [2, 41–43]. This simple application has been used also to study the relative merits of the Galerkin and collocation methods in the enforcement of the boundary and inter-element continuity conditions [33, 46].

Hybrid-Trefftz stress and displacement elements have been applied in the elastostatic analysis of stretching plates [22, 23, 25, 28, 34] and in the determination of stress intensity factors in cracked plates [25, 31, 32, 44, 45]. Still in the context of elastostatics, extensions into shape optimisation of stretching plates and into the analysis of bending plates and of solids are reported in [3, 11, 12, 21, 27, 29, 30, 47]. Hybrid-Trefftz elements have also been applied to elastoplastic analysis of plates and solids with and without strain localisation [3–5, 35, 36, 55] and to the elastodynamic analysis in the frequency domain of bounded and unbounded homogeneous and two-phase media [2–5, 7, 11, 12, 18, 19, 22–24, 27–33, 36, 41–47]

A selected number of these applications are presented below.

6.1. Convergence of alternative hybrid formulations and models

The rectangular cracked plate shown in Fig. 1, with constant modulus of elasticity, E, and Poisson ratio $\nu = 0.3$, is used in [20] to illustrate the relative rates of convergence of the alternative finite element formulations and models. The hybrid-Trefftz (HT) and hybrid (H) formulations are implemented on the mesh with six triangular elements and the hybrid-mixed (HM) formulation is implemented on the mesh with six rectangular elements. Polynomial bases are used in all tests reported in Fig. 2, for both displacement (D) and stress (S) models.

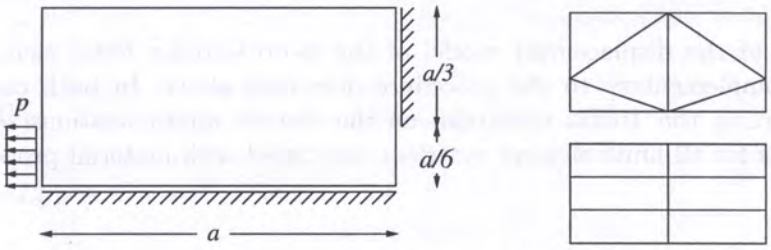

Fig. 1. Symmetric part of cracked plate and finite element meshes

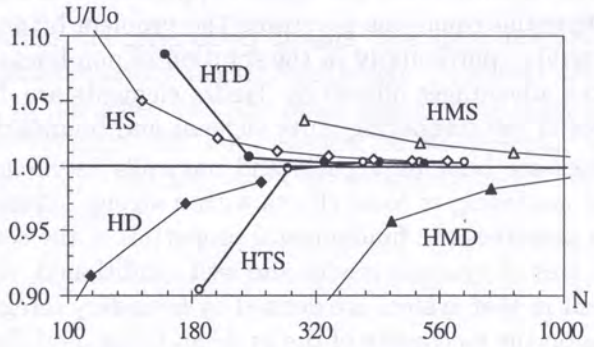

Fig. 2. Convergence of the strain energy

The convergence of the solution is studied in terms of the evolution of the strain energy, U, with the total number of degrees of freedom, N. The strain energy is normalised to the "exact" value $U_0 = 0.04584029\,(pa)^2/E$ obtained in [52] applying a dual extrapolation technique to two series of statically and kinematically admissible solutions, which provide upper and lower bounds to the exact solution, respectively.

With the hybrid-Trefftz solutions, the number of degrees of freedom needed to attain an error under one percent is relatively low, $N \approx 200$. These solutions are obtained with a polynomial basis that satisfies locally the domain equilibrium (1), compatibility (2) and elasticity (3) conditions written for static analysis. Neither of the solutions shown in Fig. 2 is strictly statically or kinematically admissible, as the Neumann and Dirichlet conditions are weakly enforced in the stress (HTS) and displacement (HTD) models, respectively. As it is mentioned below, the rate of convergence can be improve substantially by enriching the basis with local solutions associated with the singular stress field developing at the crack tip.

The hybrid stress (HS) and hybrid displacement (HD) models are derived, in general, under the constraint of satisfying locally the equilibrium (1) and compatibility (2), respectively. However, the solution sequences shown in Fig. 2 are strictly statically and kinematically admissible, as the Neumann (4) and Dirichlet (5) are also satisfied locally by the HS and HD solution sequences, respectively. Consequently, the solutions require basically the same number of degrees of freedom to attain the same error in the energy estimate.

The number of degrees of freedom needed to attain the one percent level of precision with the hybrid-mixed models is larger, $N \approx 700$, as their solutions derive from approximation bases that do not satisfy locally any of the fundamental conditions of the problem. The results shown in Fig. 2 may suggest the conclusion that the hybrid-mixed elements are the less effective. However, measurement of the efficiency in the estimate of the strain energy cannot be based directly on the dimension of the solving system. Because of the simplicity of the approximation functions, pre-processing of a hybrid-mixed element is, in general, much faster than that of any other type of element. The efficiency of the solvers depends rather more on the structure of the system and on the number of non-zero coefficients than on its dimension. Because of their different levels of sparsity, the number of non zero coefficients in a hybrid or hybrid-Trefftz system can be of the same order of magnitude of what is found in a hybrid-mixed system much larger in dimension.

The results collected in Fig. 2 are useful also to analyse the bounding nature of the solutions, which relates directly with the level of enforcement of conformity present in each solution sequence. The hybrid-Trefftz stress and displacement sequences illustrate the patterns typical of the solutions obtained when the static and kinematic admissibility conditions are enforced weakly, respectively. On the contrary, the solutions shown for the hybrid stress and displacement models are strictly statically and kinematically admissible, respectively. Consequently, their solution sequences bound the exact energy from above and from below, respectively. The same bounding pattern is displayed by the hybrid-mixed solutions because they are obtained also with a strong enforcement of the boundary conditions.

6.2. Convergence of alternative Trefftz formulations and models

The tests on convergence are illustrated with the following weakly singular potential problem,

$$\nabla^2 u = 0, \tag{30}$$

$$u_{,n} = 0 \quad \text{and} \quad u_{,n}(x,-1) = 0, \tag{31}$$

$$u(+1,y) = 0 \quad \text{and} \quad u(x,+1) = 5 - 5x. \tag{32}$$

This particular problem is defined by sub-system (1)–(5) in domain $V(x,y) = [-1,+1]^2$. It is recovered by discarding all time dependent variables and by identifying the compatibility differential operator with the space gradient vector, $\boldsymbol{\mathcal{D}}^* \equiv \nabla$, and the flexibility matrix $\boldsymbol{f}$ with the identity matrix. The Laplace equation (30) corresponds to the Navier equation obtained by combination of Eqs. (1) to (3) and Eqs. (31) and (32) are the Neumann and Dirichlet condition (4) and (5), respectively.

The Trefftz elements are implemented inserting the harmonic solution set of Eq. (30) in the approximation bases (17) and (19). The boundary approximations (18) and (20) are defined on a (orthogonal) Legendre basis.

The results obtained with the HTS and HTD models, with polynomial domain and boundary bases of degree d_V and d_Γ, respectively, are shown in Figs. 3 and 4, respectively, where e is the energy error norm. Three regular meshes are used, with one, four (2×2) and sixteen (4×4) elements.

The Least-Squares Trefftz (LST) results shown in Fig. 5 are estimated from the graphs given in [40]. The HTS and HTD solutions present similar convergence patterns. The LST solutions involve fewer explicit degrees of freedom but display a progressive deterioration of the rate of convergence under the same p- and h-refinement conditions.

The HTS and HTD convergence rate increases with p-refinement. They are not significantly affected by h-refinement, with a convergence of type $e = CN^\lambda$ for this weakly singular problem, for which $\lambda \approx -0.12\, d_\Gamma$ in both the HTD and HTS solutions.

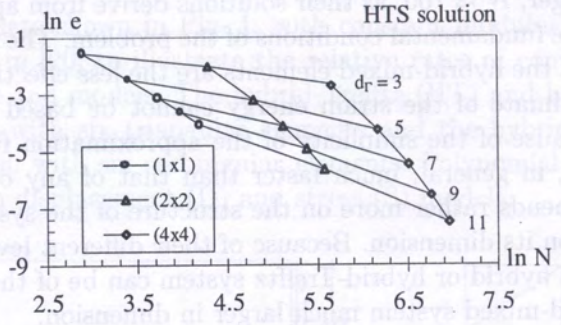

Fig. 3. Refinement of the HTS solutions ($d_V = 2d_\Gamma - 1$)

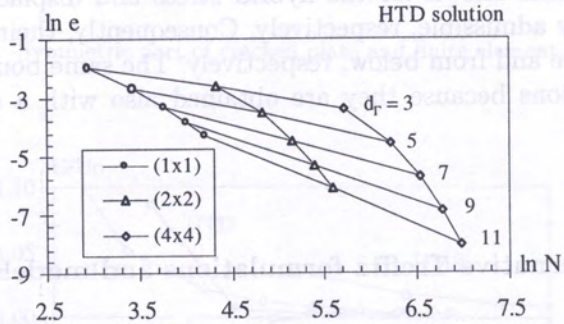

Fig. 4. Refinement of the HTD solutions ($d_V = 2d_\Gamma - 1$)

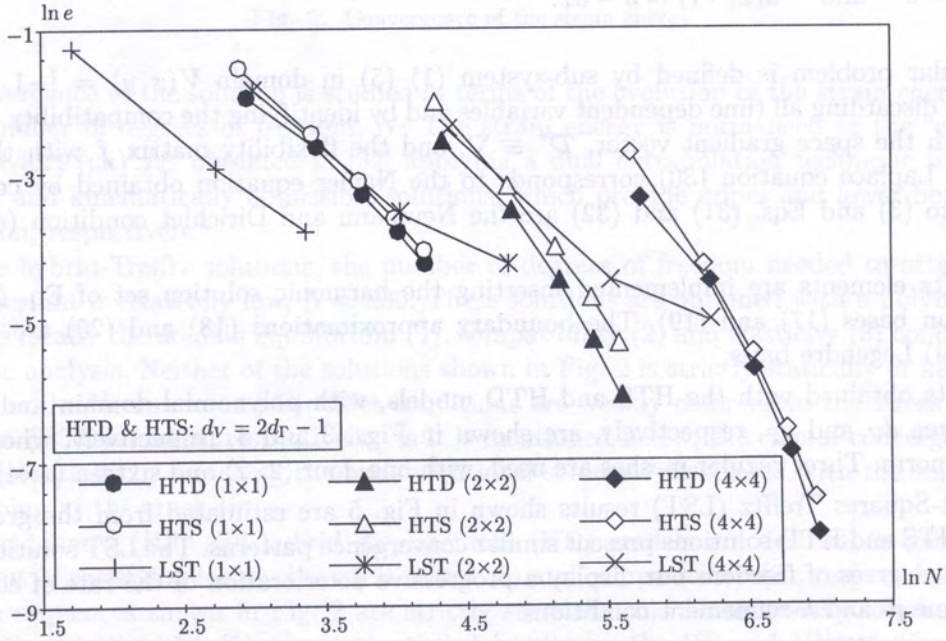

Fig. 5. Alternative hybrid-Trefftz solutions

6.3. Sensitivity to mesh distortion and incompressibility

The elastostatic problem governed by subsystem (1)–(5) is used to illustrate the sensitivity of the Trefftz finite element solutions to mesh distortion and incompressibility. The test problems, taken from [21], are three-dimensional models of straight, deep beams with cross sections shown in Fig. 6, where $b = h = L/5$ and $b' = h' = 2b$.

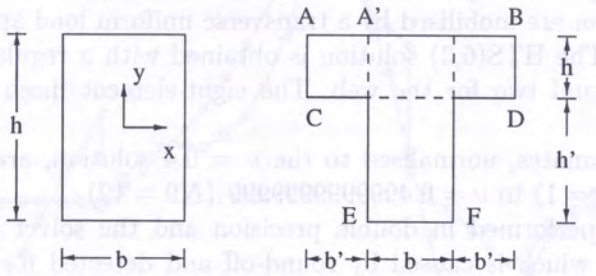

Fig. 6. Cross sections for beam tests

The test on sensitivity to mesh distortion is based on the two-element mesh cantilever beam shown in Fig. 7, with length $L = 10$, modulus of elasticity $E = 1\,500$ and Poisson ratio $\nu = 0.25$. The effect on the transverse displacement and on the axial stress at points P and Q caused by an applied moment of 4 000 is shown in Figs. 8 and 9. In these graphs, labels RGD8 and QMM identify the responses of the eight-node refined hybrid iso-parametric solid element and the modified strain variant of the incompatible brick element, respectively [6, 48, 54].

The HTS element in use is hexahedral with three-dimensional sixth degree polynomial stress fields and two-dimensional cubic boundary displacements ($d_V = 6$, $d_\Gamma = 3$). Matrix $\boldsymbol{S}_V$ present in approximation (17) is built with the linearly independent stress fields associated with the Neuber–

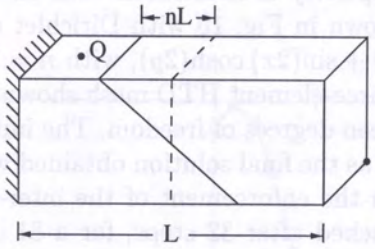

Fig. 7. Two-element mesh distortion test

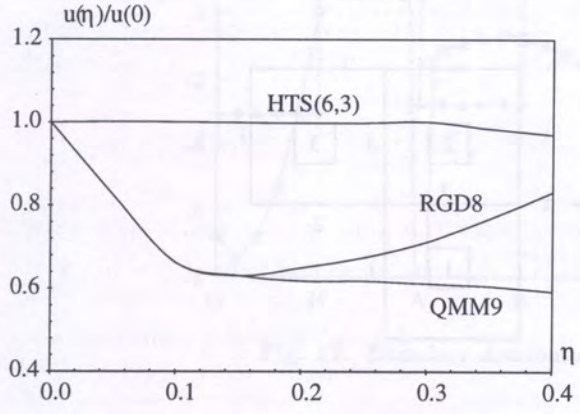

Fig. 8. Displacement sensitivity to mesh distortion

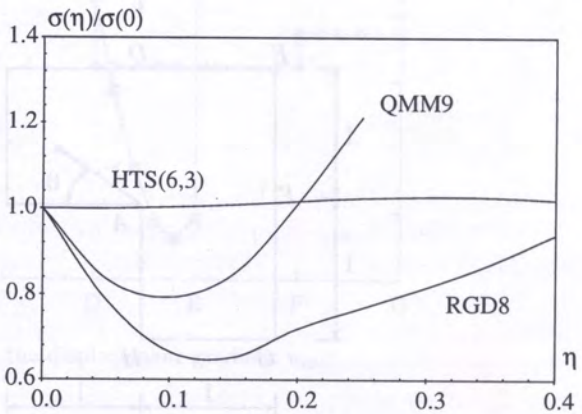

Fig. 9. Stress sensitivity to mesh distortion

Papkovitch displacement solution of the (homogeneous) Navier sub-system (1)–(3). Legendre polynomials are used to set up the boundary displacement approximation matrix $\boldsymbol{U}_\Gamma$ present in definition (18).

Insensitivity to mesh distortion is typical of the Trefftz element, in both stress and displacement variants. It has been verified that the richer is the approximation used the weaker is the sensitivity to distortions in the geometry of the finite element mesh [21, 25].

Insensitivity to incompressibility is illustrated with the T-section beam clamped at both ends. Bending, shear and torsion are mobilised by a transverse uniform load applied on flange AA' along the span length $L = 1$. The HTS(6,3) solution is obtained with a regular four-element mesh, one element for each flange and two for the web. The eight-element mesh is obtained by mid-span splitting.

The strain energy estimates, normalised to the $\nu = 0.4$ solution, are shown in Table 1. They range from $\nu = 0.49$ ($N9 = 1$) to $\nu = 0.4999999999999$ ($N9 = 12$).

The calculations are performed in double precision and the solver is adapted to detect and solve linear dependency, which is caused by round-off and detected for $N9 = 10$ and $N9 = 12$, respectively for the four- and eight-element meshes. The HTD element displays a similar insensitivity to incompressibility [25].

Table 1. Normalised strain energy in the incompressibility test

N9	1	3	5	7	8	9	10	11	12
4 FE	1.0226	1.0247	1.0247	1.0247	1.0247	1.0248	1.1287	1.0285	0.6690
8 FE	1.0181	1.0197	1.0197	1.0197	1.0197	1.0198	1.0174	1.0151	0.9012

6.4. Adaptivity

The procedure for automatic p-adaptivity is illustrated with the singular potential problem (30) defined on the L-shaped domain shown in Fig. 10 with Dirichlet conditions on sides AB and AH. The exact solution is $u = r^n \sin(n\theta) + \sin(2x)\cosh(2y)$, with $n = 2/3$ and $0 \leq \theta \leq 3\pi/2$.

The problem is solved with the three-element HTD mesh shown, with a starting polynomial basis $(d_V, d_\Gamma) = (1, 0)$ for a total of thirteen degrees of freedom. The initial and exact boundary solutions are shown in Figs. 11 and 12, as well as the final solution obtained with a p-adaptive procedure based on the minimisation of the error on the enforcement of the inter-element and Dirichlet continuity conditions. The final solution is reached after 32 steps, for a 81 degree of freedom approximation with $d_V = 11$, 7 and 9 in elements 1, 2 and 3 and $d_\Gamma = 4$, 6, 4 and 6 on boundaries 1 to 4.

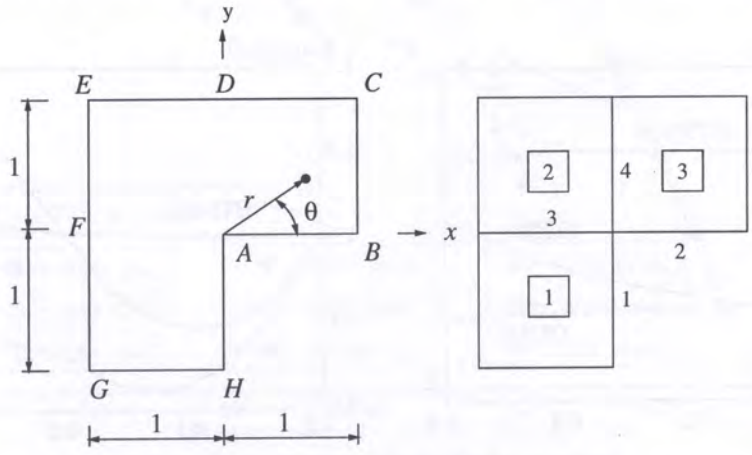

Fig. 10. Geometry and finite element mesh for the L-shaped domain

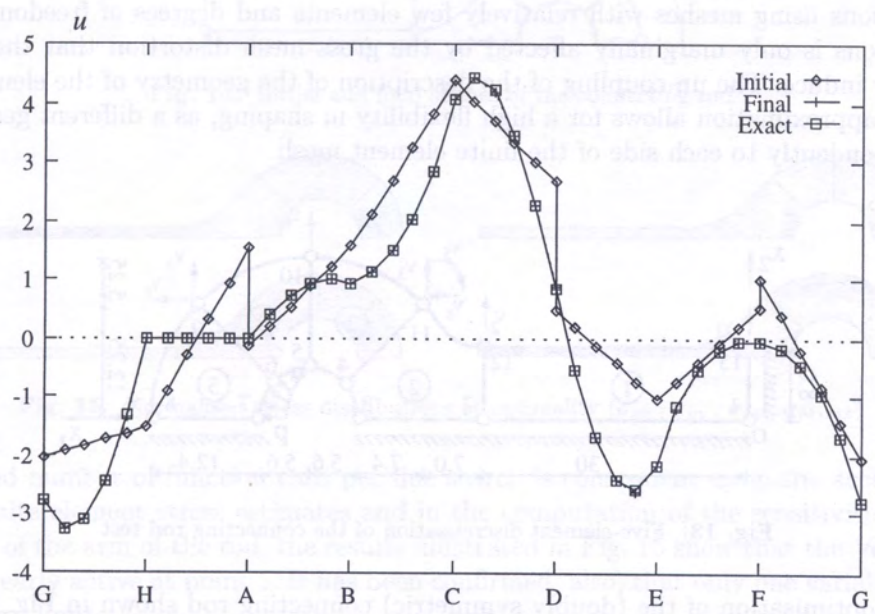

Fig. 11. Boundary distribution of the displacement u

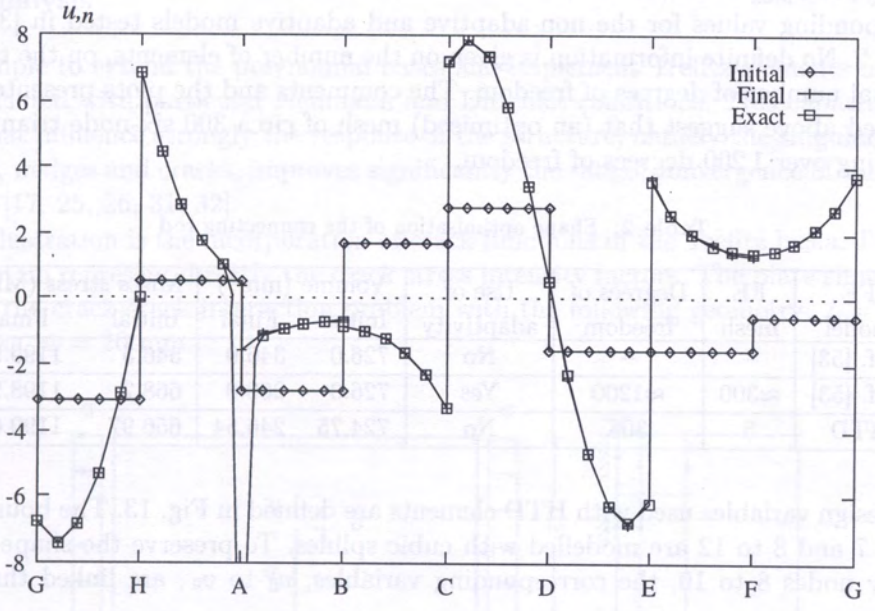

Fig. 12. Boundary distribution of the displacement gradient $u_{,n}$

6.5. Shape optimisation

Trefftz elements are particularly well suited to shape optimisation as they can produce highly accurate solutions using meshes with relatively few elements and degrees of freedom. The quality of these solutions is only marginally affected by the gross mesh distortion that the optimisation procedure may induce. The un-coupling of the description of the geometry of the elements from the finite element approximation allows for a high flexibility in shaping, as a different geometry can be assigned independently to each side of the finite element mesh.

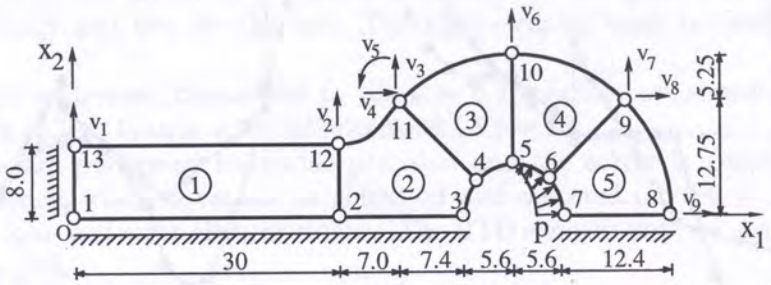

Fig. 13. Five-element discretisation of the connecting rod test

The shape optimisation of the (doubly symmetric) connecting rod shown in Fig. 13 is used frequently to assess the performance of different finite element models and mathematical programming algorithms. The initial dimensions are taken from Sienz and Hinton [53]. The plate is 1 mm thick, and the values used for the applied load, the Poisson ratio, the modulus of elasticity and the Mises stress are: $p = 500$ N/mm, $\nu = 0$, $E = 2.1 \cdot 10^6$ MPa, $\sigma_{\text{Max}} = 1200$ MPa.

This problem is solved in [27] with the mesh shown in Fig. 13 built with five hybrid-Trefftz displacement elements. The degrees in the displacement and traction approximations are $d_V = 11$ and $d_\Gamma = 5$, respectively, for a total of 308 degrees of freedom. For the discretisation shown in Fig. 13, the initial surface area is $\Omega_0 = 7247.5$ mm^2 and the maximum Von Mises stress found for the initial shape is $\sigma_{\text{Max}} = 656.97$ MPa.

The corresponding values for the non-adaptive and adaptive models tested in [37, 53] are also given in Table 2. No definite information is given on the number of elements, on the type of element and on the total number of degrees of freedom. The comments and the plots presented in the references mentioned above suggest that (an optimised) mesh of circa 300 six-node triangular elements is used, involving over 1 200 degrees of freedom.

Table 2. Shape optimisation of the connecting rod

FE model	FE mesh	Degrees of freedom	Use of adaptivity	Volume (mm^3)		Mises stress (MPa)	
				Initial	Final	Initial	Final
Ref. [53]	–	–	No	726.0	346.0	546.5	1199.9
Ref. [53]	≈300	≈1200	Yes	726.0	268.0	668.2	1198.9
HTD	5	308	No	724.75	246.54	656.97	1199.03

The nine design variables used with HTD elements are defined in Fig. 13. The boundaries defined by nodes 3 to 7 and 8 to 12 are modelled with cubic splines. To preserve the shape of the boundary defined by nodes 8 to 10, the corresponding variables, v_6 to v_9, are linked through equality constraints.

The final shape and the associated stress fields obtained controlling the Von Mises stress at sixty boundary points are shown in Figs. 14 and 15. The final shape is obtained directly from the initial design in one optimisation phase and after six iterations and six function evaluations in the connecting rod tests.

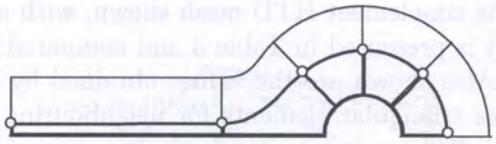

Fig. 14. Initial and final shapes of the connecting rod

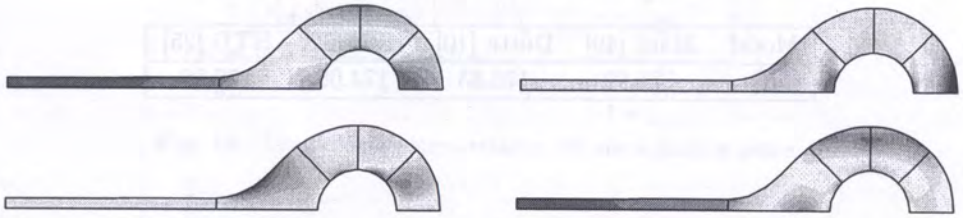

Fig. 15. Normalised stress distributions at optimality (σ_{xx} , σ_{yy} , σ_{xy} , σ_{Mises})

The reduced number of function calls per line search is consequent upon the accuracy achieved both in the finite element stress estimates and in the computation of the sensitivities. Besides the fully stressing of the arm of the rod, the results illustrated in Fig. 15 show that the Von Mises stress constraint is nearly active at point 5. It has been confirmed, also, that only one variable, v_5 , reaches the lower design limit.

E. Hinton and his co-workers use B-splines and control the shape through four primary design variables (v_1 , v_9 and the radial resultants of v_3 and v_4 and v_7 and v_8 , respectively) and six secondary variables (extended to include v_2 and v_6). The optimum shape is obtained in two steps. Once the volume is reduced for an intermediate shape, the moving limits are relaxed and the optimum shape is obtained after two iterations in the optimisation process. Hinton and his-coworkers report convergence after 15 major iterations and 42 function evaluations.

6.6. Crack analysis

It is rather simple to extend the polynomial bases and implement Trefftz elements using analytical solutions associated with particular Neumann and Dirichlet conditions. This capacity of modelling local effects that influence strongly the response of the structure, namely the singular fields induced by point loads, wedges and cracks, improves significantly the rate of convergence of the finite element solutions, e.g. [17, 25, 26, 31, 32].

A typical illustration is the incorporation of crack functions in the Trefftz basis. Their weights in the solving system represent directly the crack stress intensity factors. The plate shown in Fig. 16 is used to study the crack-crack interaction problem with the following geometry: $L = 3w$, $a = 0.5w$, $l = \delta = 0.0125w$, $w = 20$ mm.

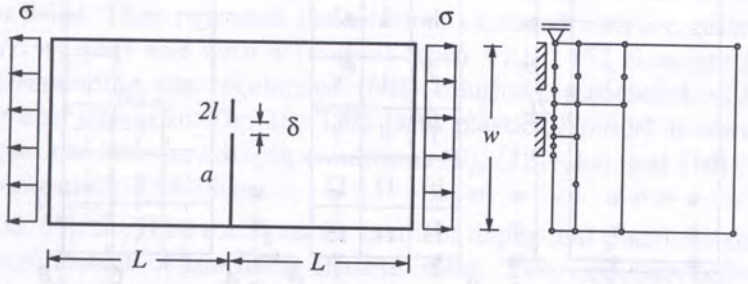

Fig. 16. Plate with two neighbouring cracks ($E = 1$ MPa, $\nu = 0.3$)

The plate is solved with the six-element HTD mesh shown, with $d_V = 13$, $d_\Gamma = 5$ and $N = 499$ degrees of freedom. The result is presented in Table 3 and compared with a 14-element HTS mesh ($d_V = 8$, $d_\Gamma = 4$, $N = 714$). Also shown are the values obtained by Maiti [49] with a 93-element, 294-node mesh, which includes triangular elements for neighbouring singularities, an extension of the earlier work of Dutta et al. [10] on singularity elements.

Table 3. Estimates for the stress intensity factor ($\mathrm{Nmm}^{-3/2}$)

Model	Maiti [49]	Dutta [10]	HTS [32]	HTD [25]
K_I	171.90	176.83	174.08	172.98

6.7. Elastoplastic analysis

Extension into non-linear and time dependent problems is simplified by the option of deriving the Trefftz models directly from the fundamental relations of the problem under analysis. For instance, to extend the formulation to elastoplasticity it suffices to add to the (unchanged) finite element equations modelling system (1)–(6) the new set of finite element equations needed to model the plastic phase of the structural response, as described by system (7)–(16).

This extension of the hybrid-Trefftz formulation reported in [35, 36, 55] is illustrated with the plane strain, Mises plate subject to a uniform displacement shown in Fig. 17, which has been used by different authors to test the gradient dependent softening plasticity model of Mühlhaus and Aifantis [50].

The basic stress approximation (17) is implemented in each element of the 15-element mesh shown in Fig. 17, and the boundary displacement approximation (18) is enforced on each element side, in both directions, except on edge AB, where only the horizontal component of the displacement field is assumed.

A plastic cell mesh is superimposed onto the finite elements selected as critical, the elements where plastic strains may develop during the loading process. The plastic multiplier field is approximated in each cell and the plastic radiations are also approximated on the boundaries of the plastic cell mesh, as stated by Eqs. (21) and (22). In the present application, the plastic multiplier field is assumed to be bilinear and non-negative, to satisfy the plastic flow condition (10), and the plastic radiation is assumed constant.

The load-displacement relations and the deflected shape of the plate in the post-collapse phase shown in Figs. 18 and 19 are obtained with the 15-element mesh with four (2×2) plastic cells per element. The number of finite element degrees of freedom involved in approximations (17) and (18)

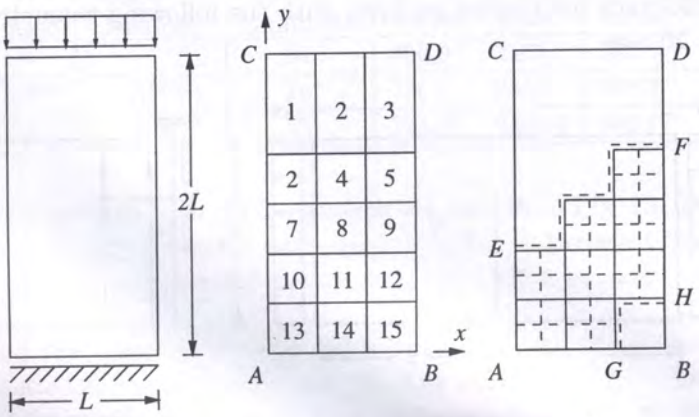

Fig. 17. Rectangular softening plate subject to a uniform displacement

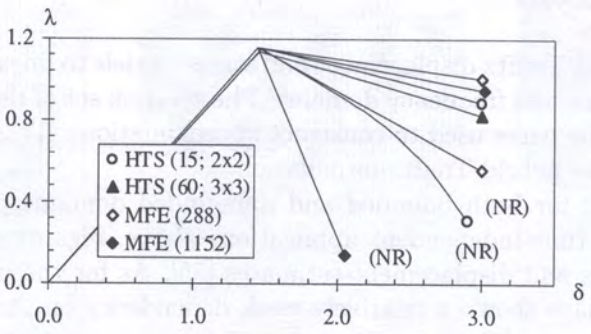

Fig. 18. Load-displacement relation for the softening plate

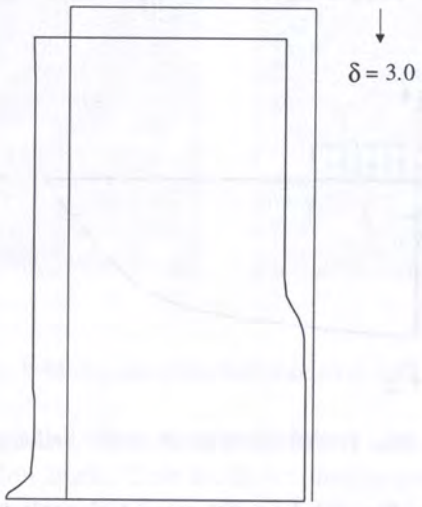

Fig. 19. Deflected shape of the rectangular plate

is $N_{FE} = 745$ and corresponds to seventh degree stresses and cubic displacements. The number of degrees of freedom in the plasticity approximations (21) and (22) is $N_* = 206$.

The load and the displacement are scaled to the yield stress $\sigma = 100$ MPa and to $L\sigma/E$, respectively, with $E = 11\,920$ MPa and $L = 60$ mm. The plastic softening and diffusion coefficients used are $h = 400$ MPa and $c = 3\,600$ N. Also shown in Fig. 18 is the refined solution obtained by subdividing each element in four elements (60-element mesh, $N_{FE} = 2\,900$) and taking nine (3×3) plastic cells per element associated with a maximum $N_* = 427$ active plastic variables.

The sequences of solutions labelled MFE are taken from [9]. They are obtained with a mixed finite element model based on the direct approximation of the displacement, stress, elastic strain and plastic multiplier fields. They represent the solutions obtained with a regular 288-element mesh ($N_{FE} = 1\,039$ and $N_* = 163$) and with a (biased) mesh with 1 152 elements ($N_{FE} = 8\,037$ and $N_* = 576$). The corresponding non-regularised (NR) solutions, associated with the conventional plasticity model, are also shown in Fig. 18. This local plasticity model is obtained by removing the finite element equations associated with conditions (9), (12)–(14) and (16). The finite element solutions become clearly mesh-dependent.

As it is shown in [35, 55], the HTS solutions for gradient dependent plasticity problems are weakly dependent on the h-refinement of the finite element mesh. They produce high quality estimates for the stress, strain and displacement fields in both pre- and post-collapse phases, and describe accurately the process of gradual propagation of plasticity, both in terms of the geometry of the shear band (slope and width) and of the deformation fields.

6.8. Elastodynamic analysis

The extension of the hybrid-Trefftz displacement and stress models to linear elastodynamic problems has been tested in both time and frequency domains. The solution set of the governing wave equation is now used to establish the bases used to construct approximations (17) and (19) of the stress and displacement models of the hybrid-Trefftz formulation.

The solutions obtained for both bounded and unbounded domains preserve the basic characteristics reported for the time-independent applications above, regarding sensitivity to distortion and accuracy of the stress and displacement estimates [55]. As for the plasticity applications, the elastodynamic solutions have shown a relatively weak dependency on the mesh refinement, now in terms of the exciting frequency [7].

The HTD element is used to analyse the elastic half-space subject to a harmonic distributed load of intensity $p = 1$ N/m^2 shown in Fig. 20. The values used for the mass, the Lamé constants and the P-wave velocity are $\rho = 1621.8$ kg/m^3, $\lambda = 0.223733$ GN/m^2, $\mu = 0.1119$ GN/m^2 and $c_1 = 525.308$ m/s, respectively.

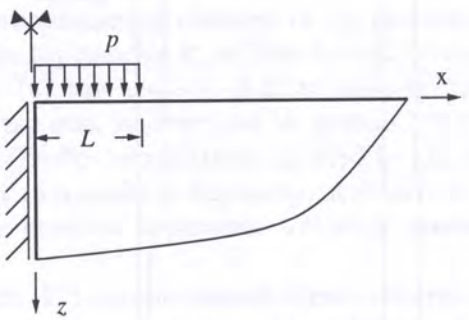

Fig. 20. Forced vibration of elastic half-space

The different meshes shown in Fig. 21 have been tested with the purpose of obtaining, in the same program run, accurate estimates for stresses and displacements in both near- and far-field ranges. They differ, essentially, in two aspects, namely the refinement of the mesh under the applied load and the enforcement of the Sommerfeld diffusivity condition. The first technique used to model this condition consists in using a bounded mesh with an absorbing boundary placed at distance r_0 in Fig. 21. The second technique consists in implementing the mesh with one unbounded element (domain $r_0 \leq r < \infty$ in the same figure) built on an approximation basis that satisfies locally the Sommerfeld condition. Part of the results reported in [7] are presented in Figs. 22 and 23.

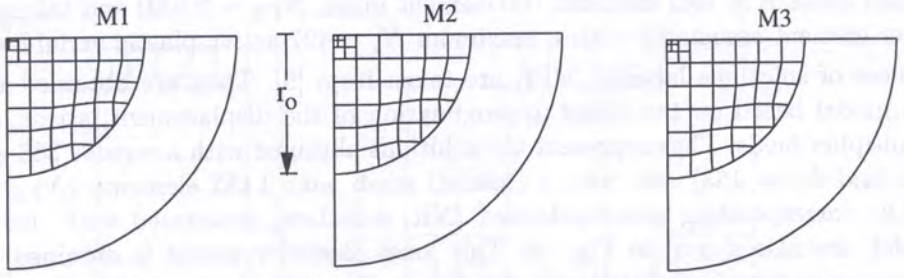

Fig. 21. Meshes used in the tests with hybrid-Trefftz displacement elements

Figure 22 shows the far-field displacement distribution for a wide range of forcing frequencies using the same mesh built with forty hybrid-Trefftz displacement finite elements. The domain shown in Fig. 22 is bounded by coordinates $x_{\max} = z_{\max} = 50L$, where L is the length of the applied load. It is seen that the P-wave travelling along the axis of symmetry is clearly depicted, as well as the

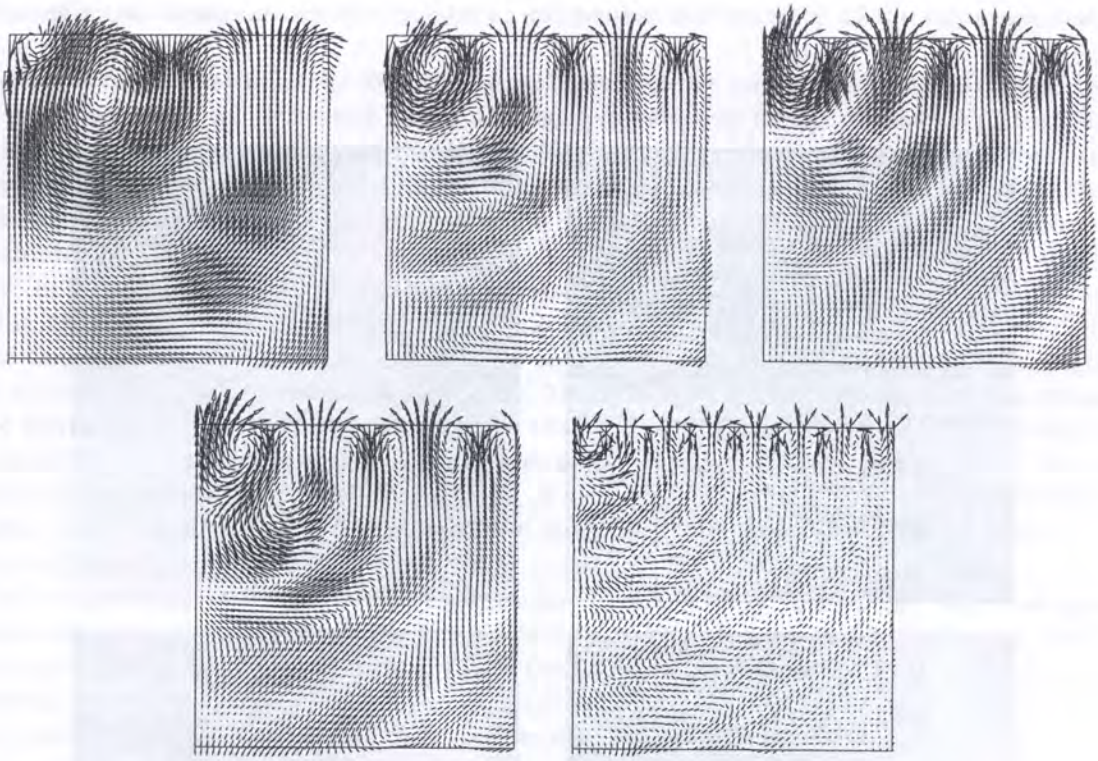

Fig. 22. Far-field displacement field modelled with HTD elements

S-wave travelling with a 45° gradient. Also clearly modelled is the surface Rayleigh wave, which is not included in the approximation basis. This basis is constructed with the hierarchical Bessel and Hankel solutions of the wave equation for bounded and unbounded elements, respectively.

Figure 23 shows the HTD near-field stress distribution ($x_{\max} = z_{\max} = 5L$) obtained with the same fourty-element mesh, which involves a total of 3 250 degrees of freedom. It is compared with the solution obtained with a refined mesh of 40 400 elements CPE4 (bounded) and CINPE4 (unbounded) offered in the ABAQUS library [1], involving a total of 81 604 degrees of freedom. It is seen clearly that the (unsmoothed) HTD solution satisfies the Neumann condition with far better precision than that obtained with the refined (and smoothed) ABAQUS solution.

7. Closure

The hybrid-Trefftz finite formulation reported in this paper should not be understood as the result of an autonomous approach to the finite element method. It represents, instead, the most constrained set of a wider and coherently inter-related family of hybrid finite element formulations.

Four basic ideas have been exploited to establish this framework for the alternative formulations and models for the finite element method. They consist in deriving the finite element formulations and models from the relevant first principles, in coupling the finite element mappings with duality and in processing the resulting solving systems by mathematical programming. The fourth basic ingredient is the systematic use of generalised finite element variables.

The role of mathematical programming is two-fold, namely to establish the theoretical framework of the formulations and models and (eventually) to provide the necessary numerical solution procedures. The variational statements associated with a particular formulation and model are derived a posteriori by establishing and interpreting the mathematical programs equivalent to the finite element solving system. Mathematical programming theorems are used also to es-

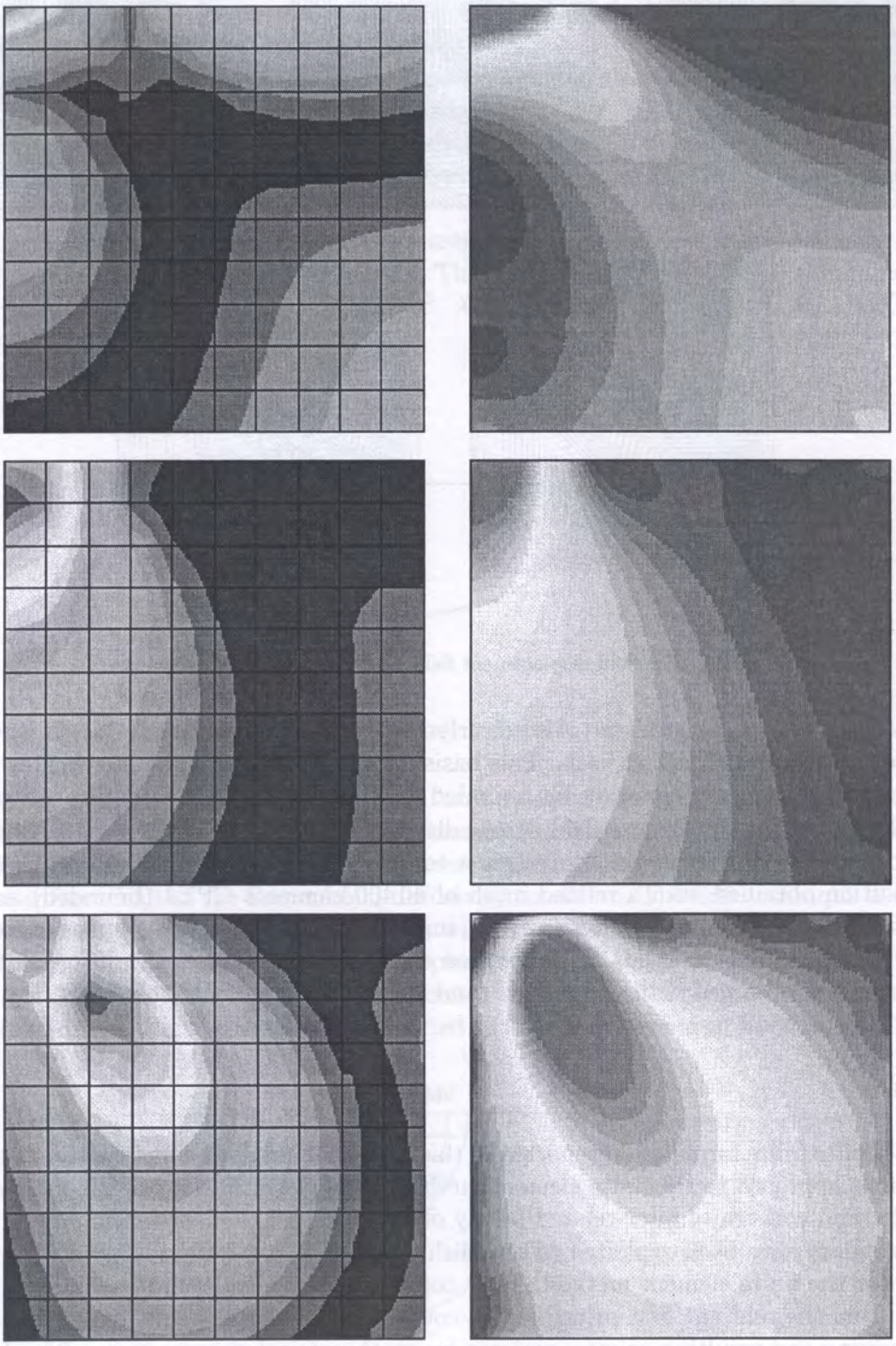

Fig. 23. Near-field stresses (σ_{xx} , σ_{yy} , σ_{xy}) obtained with ABAQUS elements (left) and HTD elements (right)

tablish sufficient conditions for the existence, uniqueness and stability of the finite element solutions.

Duality is the equivalent to the condition on invariance of the inner product in all (time and space) mappings involved in the derivation of a particular finite element model. Duality is instrumental in the identification of the conditions that should be enforced on average and of the respective laws of enforcement. By ensuring the definition of energetically consistent finite element variables and equations, duality preserves in the finite element representation the fundamental properties of the problem being modelled.

The option of deriving the hybrid-Trefftz elements from the relevant first principles, instead of using existing or newly coined variational statements, proved to be essential to establish their nature and their relationship with alternative or equivalent finite element models, in particular those derived by J. Jirousek and his co-workers. Yet another development has been the systematic use of hierarchical (and orthogonal, whenever possible) approximation functions in detriment of the conventional nodal polynomial bases. Besides enhancing the p-adaptive and parallel processing features of the resulting finite element models, it also allows implementation of alternative, independent, highly accurate discretisation in time and space and facilitates their application in the solution of non-linear problems.

The major strength of Trefftz elements resides in their ability to combine the most interesting features of the conventional finite element and boundary element methods, namely symmetric (when applicable) and sparse solving systems described by boundary integral expressions. Their low sensitivity to mesh distortion and incompressibility and the higher convergence rates they offer result, mainly, from the richness of the approximation bases they are derived from. The price paid to achieve these features is the higher complexity of the approximation functions being used and, mainly, a relatively higher problem-dependency.

It is hoped that the results reported here may help to question the generalised perception that the domain of competitiveness of hybrid-Trefftz elements is restricted to the solution of linear problems. Presently, they deserve fully to be accepted as special-purpose, high-performance finite elements. Hybrid-Trefftz elements are still in a relatively early stage of development. They may never evolve to reach the status of all-purpose finite elements, unless the development in hardware justifies the investment in a new generation of computer codes. This follows from the fact that specially designed implementation techniques must be used to exploit fully the main features these elements offer. A relevant number of these features, including some of those responsible for the highest levels in competitiveness of hybrid-Trefftz elements, are inhibited when these elements are implemented by borrowing and adapting directly the techniques and tools developed for the conventional conforming finite element.

Acknowledgement

Part of the applications used in this paper have been developed by research students I. Cismaşiu, F.L.S. Bussamra and Z.M. Wang, as referenced in the text. This work has been developed at ICIST, Instituto Superior Técnico, and has been supported by Fundação para a Ciência e Tecnologia through research contracts established in the framework of the research funding program PRAXIS XXI.

References

[1] *ABAQUS, Standard, Version 5.7.* Hibbit, Karlsson & Sorensen, Inc., 1997.

[2] R.A. Adey, N. Kamiya, E. Kita, eds. *Trefftz method: 70 years.* Special issue, *Adv. Eng. Software*, **24**, 1995.

[3] F.L.S. Bussamra. *Hybrid-Trefftz Stress Elements: a Three-Dimensional Model for Elastoplasticity* (in Portuguese). Ph.D. thesis, Universidade de São Paulo, Brazil, 1999.

[4] F.L.S. Bussamra, P.M. Pimenta, J.A.T. Freitas. Three-dimensional elastoplastic analysis with hybrid-Trefftz stress elements (in Portuguese). In: P.M. Pimenta, ed., *Proc. 20th CILAMCE*, São Paulo, Brazil, 1999.

[5] F.L.S. Bussamra, P.M. Pimenta, J.A.T. Freitas. Hybrid-Trefftz stress elements for three-dimensional elastoplasticity. 2nd Int. Workshop Trefftz Method, Sintra, 1999.

[6] W. Chen, Y.K. Cheung. Three-dimensional 8-node and 20-node refined hybrid isoparametric elements. *Int. J. Num. Meth. Engng.*, **35**: 1871–1889, 1992.

[7] C. Cismaşiu. *The Hybrid-Trefftz Displacement Element for Static and Dynamic Structural Analysis Problems.* Ph.D. thesis, Technical University of Lisbon, Portugal, 2000.

[8] I. Cismaşiu, J.P.M. Almeida, L.M.S.S. Castro, D.C. Harbis. Parallel solution techniques for hybrid-mixed finite element models. In: M. Papadrakakis, B.H.V. Topping, eds., *Innovative Computational Methods for Structural Mechanics.* Saxe-Coburg Publications, 1999.

[9] C. Comi, U. Perego. A generalized variable formulation for gradient dependent softening plasticity. *Int. J. Num. Meth. Engng.*, **39**: 3731–3755, 1997.

[10] B.K. Dutta, S.K. Maiti, A. Kakodkar. On the use of one point and two points singularity elements in the analysis of kinked cracks. *Int. J. Num. Meth. Engng.*, **29**: 1487–1499, 1990.

[11] C.M.T.T. Fernandes, V.M.A. Leitão. On a least squares Trefftz collocation method for plate bending. *J. Mech. Eng.*, **50**: 387–397, 1999.

[12] C.M.T.T. Fernandes, V.M.A. Leitão, A. Vásárhelyi. Thin plate bending analysis using an indirect Trefftz collocation method. *CAMES*, **8**: 1–16, 2001.

[13] J.A.T. Freitas. Duality and symmetry in mixed integral methods of elastostatics. *Int. J. Num. Meth. Engng.*, **28**: 1161–1179, 1989.

[14] J.A.T. Freitas. Variational theorems in elastoplastic boundary element analysis. In: C.A. Brebbia, J.J. Connor, eds., *Advances in Boundary Elements*, **3**: 65–79, Computational Mechanics Publications, 1989.

[15] J.A.T. Freitas. Mixed and hybrid symmetric formulations for the boundary integral method. *Eur. J. Mech. A/Solids*, **9**: 1–20, 1990.

[16] J.A.T. Freitas. A kinematic model for plastic limit analysis of solids by the boundary integral method. *Comput. Meth. Appl. Mech. Eng.*, **88**: 189–205, 1991.

[17] J.A.T. Freitas. Formulation of elastostatic hybrid-Trefftz stress elements. *Comp. Meth. Appl. Mech. Eng.*, **153**: 127–151, 1997.

[18] J.A.T. Freitas. Hybrid-Trefftz displacement and stress elements for elastodynamic analysis in the frequency domain. *CAMES*, **4**: 345–368, 1997.

[19] J.A.T. Freitas. Hybrid finite element formulations for elastodynamic analysis in the frequency domain. *Int. J. Solids Struct.*, **36**: 1883–1923, 1999.

[20] J.A.T. Freitas, J.P.M. Almeida, E.M.B.R. Pereira. Non-conventional formulations for the finite element method. *Comput. Mech.*, **23**: 420–429, 1999.

[21] J.A.T. Freitas, F.L.S. Bussamra. Three-dimensional hybrid-Trefftz stress elements. *Int. J. Num. Meth. Engng.*, **47**: 927–950, 2000.

[22] J.A.T. Freitas, C. Cismaşiu. Formulation of hybrid-Trefftz displacement elements. In: Topping BHV, ed., *Advances in Finite Element Technology.* Civil-Comp Ltd, 1996.

[23] J.A.T. Freitas, C. Cismaşiu. Implementation of hybrid-Trefftz displacement elements. In: B.H.V. Topping, ed., *Advances in Finite Element Technology.* Civil-Comp Ltd, 1996.

[24] J.A.T. Freitas, C. Cismaşiu. Hybrid-Trefftz displacement element for spectral analysis of bounded and unbounded media. Int. Rept., ICIST, Instituto Superior Técnico, 1998.

[25] J.A.T. Freitas, C. Cismaşiu. Numerical implementation of hybrid-Trefftz displacement elements. *Comput. and Struct.*, **73**: 207–225, 1999.

[26] J.A.T. Freitas, C. Cismaşiu, Z.M. Wang. Comparative analysis of hybrid-Trefttz stress and displacement elements. *Arch. Comput. Meth. Engng.*, **6**: 35–59, 1999.

[27] J.A.T. Freitas, I. Cismaşiu. Shape optimization with hybrid-Trefftz displacement elements. *Int. J. Num. Meth. Engng.* (submitted for publication).

[28] J.A.T. Freitas, Y.F. Dong. Implementation of Michell's polynomial stress functions in hybrid finite element codes. In: Y.J. Zhang, ed., *EPMESC IV*, Dalian Univ. Tech. Press, 1992.

[29] J.A.T. Freitas, Z.Y. Ji. Hybrid-Trefftz stress elements for thin plate bending analysis. Int. Rept., ICIST, Instituto Superior Técnico, 1995.

[30] J.A.T. Freitas, Z.Y. Ji. Hybrid-Trefftz stress elements for plate bending analysis. Int. Rept., ICIST, Instituto Superior Técnico, 1995.

[31] J.A.T. Freitas, Z.Y. Ji. Hybrid-Trefftz boundary integral formulation for the simulation of singular stress fields. *Int. J. Num. Meth. Engng.*, **39**: 281–308, 1996.

[32] J.A.T. Freitas, Z.Y. Ji. Hybrid-Trefftz equilibrium model for crack problems. *Int. J. Num. Meth. Engng.*, **39**: 569–584, 1996.

[33] J.A.T. Freitas, V.M.A. Leitão. A symmetric collocation Trefftz boundary integral formulation. *Comput. Mech.* (in press).

[34] J.A.T. Freitas, E.M.B.R. Pereira. Application of the Mathieu series to the boundary integral method. *Comput. and Struct.*, **40**: 1307–1314, 1991.

[35] J.A.T. Freitas, Z.M. Wang. Hybrid-Trefftz stress elements for elastoplasticity. *Int. J. Num. Meth. Engng.*, **43**: 655–683, 1998.

[36] J.A.T. Freitas, Z.M. Wang. Hybrid-mixed stress elements for gradient plasticity. In: S. Idelsohn, E. Oñate, E. Dvorkin, eds., *Proc. 4th World Cong. Computational Mechanics*, Buenos Aires, Argentina, 1998.

[37] E. Hinton, J. Sienz, B. Hassani. Fully integrated design optimization for engineering structures with benchmarking. In: B.H.V. Topping, ed., *Advances in Structural Engineering Optimization*, Civil-Comp Ltd, 1996.

[38] J. Jirousek, N. Leon. A powerful finite element for plate bending. *Comput. Meth. Appl. Mech. Eng.*, **12**: 77–96, 1977.

[39] J. Jirousek, P. Teodorescu. Large finite element method for the solution of problems in the theory of elasticity. *Comput. and Struct.*, **15**: 575–587, 1982

[40] J. Jirousek, A. Wróblewski. Least-squares T-elements: equivalent FE and BE forms of a substructure oriented boundary solution approach. *Comm. Numer. Meth. Engng.*, **10**: 21–32, 1994.

[41] J. Jirousek, A. Wróblewski. T-elements: State of the art and future trends. *Arch. Comput. Meth. Eng.*, **3**: 323–434, 1996.

[42] J. Jirousek, A.P. Zieliński. Survey of Trefftz-type element formulations. *Comput. and Struct.*, **63**: 225–242, 1997.

[43] M. Kleiber, H. Mang, A.P. Zieliński, eds. *Trefftz method: recent developments and perspectives.* Special issue, *CAMES*, **4**/3/4, 1997.

[44] V.M.A. Leitão. On the implementation of a multi-region Trefftz-collocation formulation method for 2-D potential problems. *Engng. Anal. Boundary Elements*, **20**: 51–61, 1997.

[45] V.M.A. Leitão. Application of multi-region Trefftz-collocation to fracture mechanics. *Engng. Anal. Boundary Elements*, **22**: 251–256, 1998.

[46] V.M.A. Leitão. Comparison of Galerkin and collocation Trefftz formulations for plane elasticity. *2nd Int. Workshop Trefftz Method*, Sintra, 1999.

[47] V.M.A. Leitão, C.M.T.T. Fernandes. On a multi-region Trefftz collocation method for plate bending. In: S. Idelsohn, E. Oñate, E. Dvorkin, eds., *Proc. IV World Cong. Computational Mechanics*, Buenos Aires, 1998.

[48] X.Y. Lu, Y.W. Liu, H.R. Xu, C.X. Yao, J.T. Chen. Investigation and improvement of Wilson nonconforming element. *Acta Mech. Sinica*, **21**: 379–384, 1989.

[49] S.K. Maiti. A multicorner variable order singularity triangle to model neighbouring singularities. *Int. J. Num. Meth. Engng.*, **35**: 341–408, 1992.

[50] H.B. Mühlhaus, E.C. Aifantis. A variational principle for gradient plasticity. *Int. J. Solids Struct.*, **28**: 845–857, 1991.

[51] J. Munro, D.L. Smith. Linear programming duality in plastic analysis and synthesis. *Proc. Int. Symp. Computer Aided Structural Design*, Coventry, 1972.

[52] O.J.B.A. Pereira. *Application of equilibrium finite elements to adaptive refinement* (in Portuguese). Ph.D. thesis, Technical University of Lisbon, Portugal, 1996.

[53] J. Sienz, E. Hinton. Reliable structural optimization with error estimation, adaptivity and robust sensitivity analysis. *Comp. and Struct.*, **64**: 31–63, 1997.

[54] R.L. Taylor, P.J. Beresford, E.L. Wilson. A non-conforming element for stress analysis. *Int.J. Num. Meth. Engng.*, **10**: 1211–1219, 1976.

[55] Z.M. Wang. *Elastoplastic structural analysis with hybrid stress elements.* Ph.D. thesis, Technical University of Lisbon, Portugal, 2000.